

***In situ* surface monitoring system for synchrotron mirrors under high heat load**

Peter H. Mui, George Srajer, and Dennis M. Mills

A portable electro-optical system capable of real-time measurements of surface slope distortions down to $0.5 \mu\text{rad}$ is described; the system is limited primarily by its short-term stability. The system employs an angle measurement technique that, in combination with the least-squares signal extraction method, reduces system fluctuations. In addition, a multireflection technique is used to enhance the detectable resolution. Although designed for use with mirrors for synchrotron radiation sources, this system has the flexibility to be applied to other optical components. The prototype system has been tested on a sample mirror piece, and preliminary results are presented. A brief discussion about the extension of this metrology unit to adaptive optics is also given. © 1997 Optical Society of America

Key words: Metrology, thermally induced surface distortion, mirrors.

1. Introduction

Third-generation high-brilliance synchrotron radiation sources, such as the Advanced Photon Source, can deliver enormous x-ray power (4 kW) and power density (140 W/mm^2) to beamline optics. To harvest the brilliance of such high-power x-ray beams fully, one needs to maintain x-ray mirror surfaces with a tolerance of less than 1 arc sec ($5 \mu\text{rad}$) under these thermal loads. Currently there are commercially available metrology systems for measuring the absolute figure of these mirrors off line. However, such complex systems are massive, slow, and expensive, and only recently has an *in situ* modification of a metrology system been proposed.¹ Although other third-generation facilities, such as the European Synchrotron Radiation Facility operating in Grenoble, France, have developed *in situ* monitoring systems as part of adaptive mirror system,² the system described here is considerably more compact, portable, and less expensive than previous designs.

Knowledge of thermally induced deformations in these mirrors under high heat loading not only allows direct comparison of various cooling schemes but also provides experimental data to verify theoretical calculations. To address this critical issue, we have

developed at the Advanced Photon Source a portable electro-optical system for real-time, *in situ* monitoring of thermally induced surface slope distortions of synchrotron mirrors under high heat load. Because thermal deformations are continuous, the mirror surface is sampled at a discrete set of points to avoid the use of translating devices, which are typically heavy, slow, and expensive. Our system uses a multipass technique^{3,4} to magnify the angular deviations to within the resolution of a commercially available CCD camera with $9\text{-}\mu\text{m}$ pixels. A least-squares signal extraction method is then used to suppress the system noise and fluctuations.

Our system has been demonstrated to have an angular resolution of $\sim 0.5 \mu\text{rad}$ rms (or 0.1 arc sec) and a long-term stability better than $2 \mu\text{rad}$ over a period of 15 h. With the present camera this system is capable of sampling eight discrete points on the optic's surface profile in less than 2 min. The unit can readily be incorporated into an adaptive mirror system with the addition of a faster camera and the necessary actuator hardware.

2. Design of the System

To sample the surface deformation of the mirror, a laser beam is directed at the sites of interest, and the surface changes are monitored with either interferometric techniques or angle measurement techniques. The latter method provides only information averaged over the laser beam spots on the mirror surface, which are typically 3 mm in diameter. One can readily obtain submillimeter spatial resolution with a multipass interferometer; however, even with a high-resolution

The authors are with Advanced Photon Source, Argonne National Laboratory, Argonne, Illinois 60439.

Received 21 June 1996; revised manuscript received 28 October 1996.

0003-6935/97/225546-06\$10.00/0

© 1997 Optical Society of America

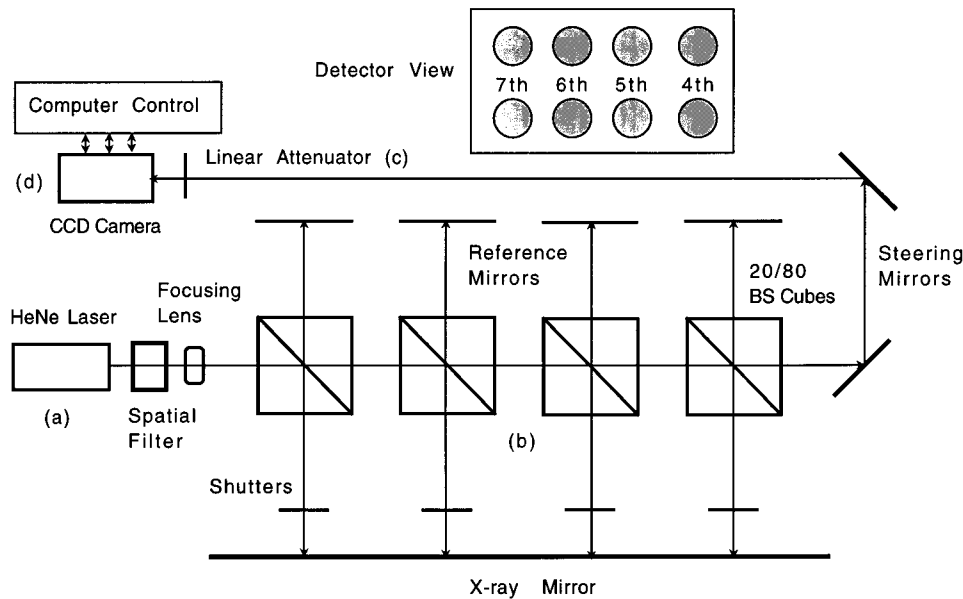


Fig. 1. Four main components of the *in situ* surface metrology unit: (a) probing light source, (b) multireflection cavities, (c) collector optics, and (d) detector and image analyzer.

array detector, the accuracy is limited to $\sim 1/200$ of the wavelength of the probing source,³ or 3 nm for a red He-Ne laser of $\lambda = 632.8$ nm. To measure a differential surface slope of 1 μ rad over a segment of less than 1 mm, one needs to determine the differential surface height with subnanometer accuracy. To obtain such high accuracy, one must also incorporate the phase-shifting or the heterodyne technique. Either implementation is very expensive and complex. Furthermore, the data-acquisition time associated with interferometry is usually much slower than that associated with the angle measurement technique because much more intensive image processing is needed.

Because the main interest is in the mirror deformations under thermal load from the x-ray beam, fine spatial resolution is not critical because thermal deformations occur on a scale comparable with the mirror's dimensions, which are typically many tens of centimeters to a meter in length. However, short profiling time (approximately seconds) is crucial because the objective is to observe the evolution of the mirror surface slope distortion. For reasons of simplicity, cost, and speed, the angle measurement approach was chosen.

3. Operation of the System

A schematic of the metrology unit is shown in Fig. 1. There are four major components: (a) a laser source with a spatial filter, (b) multireflection cavities, (c) collector optics, and (d) a CCD detector. The principle of operation is as follows: Each of the reference mirrors forms a local resonator cavity with the x-ray mirror, causing different portions of the probing laser beam to strike the mirrors a different number of times before exiting the cavity. Every time the beam reflects off the x-ray mirror, it undergoes an angular deviation equal to twice the tilt of the x-ray mirror with respect to the reference mirror. Using

the geometrical analysis illustrated in Fig. 2, one can show that, when the beam is reflected n times inside a resonator cavity, the angular deviation of the output beam is equal to $2n$ times the tilt of the x-ray mirror with respect to the reference mirror. This way one can greatly magnify the actual spatial shift

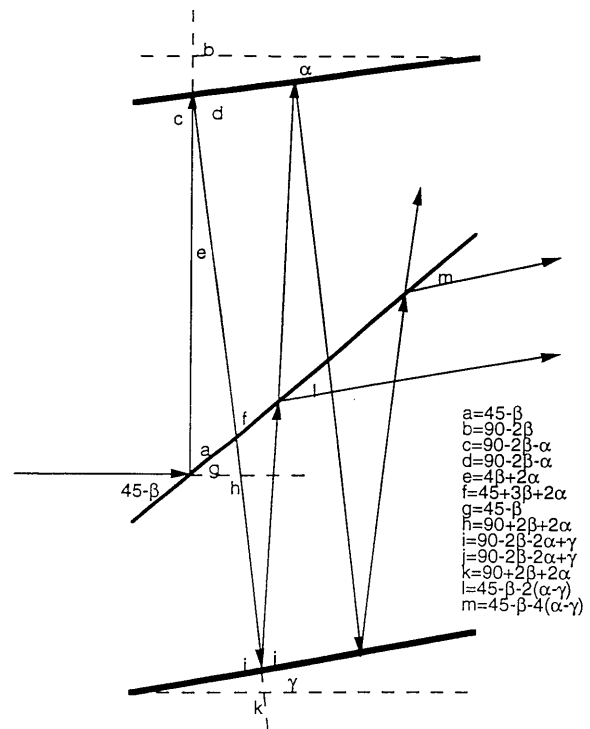


Fig. 2. Geometrical analysis, showing that when the laser beam is reflected n times in the cavity, the angular deviation of the exiting beam is $2n$ times the tilt of the x-ray mirror with respect to the reference mirror.

of the beam centroid for a given angular shift of the mirror under investigation. We selected to image the fourth, fifth, sixth, and seventh reflections to provide a resolution enhancement of approximately 10.

The probing laser beam is first low-pass filtered to reduce the ambient spatial fluctuations and then collimated by a focusing lens to reduce beam divergence. The beam-splitter cubes, reference mirrors, and steering mirrors are aligned so that, at any given time, reflections from one site (or cavity) fall on one half of the CCD camera and those from a different site fall on the other half. A linear attenuator is added to equalize the intensities of the four reflection spots to within the limited dynamic range of the CCD detector. Also, an optical (He-Ne) laser line filter is mounted inside the camera to reduce the background noise. Because of the small area of the CCD detector, mechanical shutters are needed to let us selectively observe each site. A convergent lens is used to sharply image the reflection spots onto the camera, which is centered about the focal point of the lens. For such a configuration, one can show that the location of the spot at the focal plane, in the paraxial approximation, is equal to the product of the focal length and the angle of the incident ray, independent of the initial spot location.⁵ This independence provides a consistent linear relationship between the surface slope distortions and the motion of the reflection spots. Because the sensitivity is proportional to the focal length, a plano-convex lens of long (1 m) focal length was chosen.

4. Signal Processing

A background noise profile is taken before each set of measurements and is subsequently subtracted from the image profile to reduce ambient fluctuations. The resulting picture is then processed with a low-threshold filter to sharpen each image spot and to eliminate small background fluctuations. A weighed-average routine is used to calculate the shifts of the centroid coordinates along the x and y directions. These shifts are then passed through a least-squares estimator and a high-pass filter to get the surface slope deformation along each direction. The procedure is summarized in the flow chart given in Fig. 3. The purpose and operation of the estimator and the high-pass filter are explained in the latter part of this section.

There are several sources of noise in the system: (1) the inherent quantum noise present in the CCD detector; (2) the motion fluctuations in the reference mirrors; (3) the motion fluctuations in the steering mirrors, beam splitter, attenuator, lenses, and camera; and (4) the pointing fluctuations of the laser. The quantum noise, in this case, is the easiest to deal with because, when the camera is thermoelectrically cooled, the noise in the detector for all practical purposes is negligible. One can see from Fig. 2 that a motion in the reference mirror produces an effect equivalent to a deformation on the x-ray mirror. However, with sturdy mechanical components, such drifts are typically much slower than the heat-induced deformations, allowing one to filter them out temporally. This is accomplished by subtracting

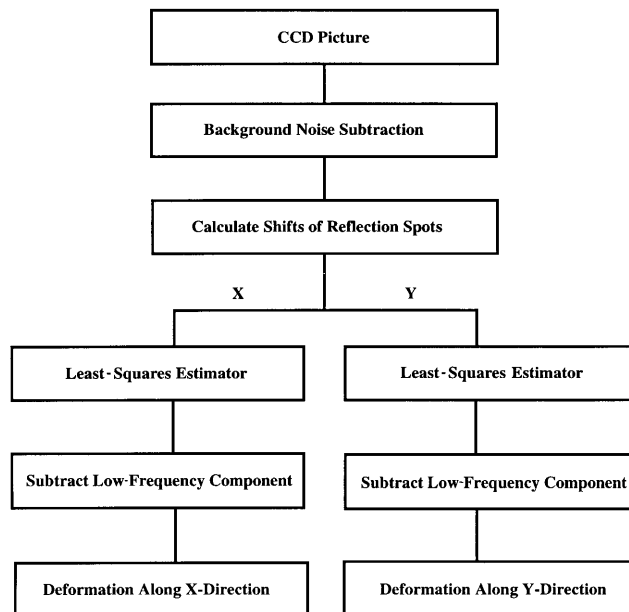


Fig. 3. Flow chart showing the signal processing algorithm.

from the low-frequency components, yielding no delay in the output information stream. The low-pass filter is a sharp digital optimal (equal-ripple) filter⁶ of length 50, which passes only the lower 10% of the frequency components. Noises (3) and (4) can be quite large, but they just shift all the reflection spots by a constant amount with respect to the CCD detector. It will be shown below how to distinguish and to eliminate such constant shifts with the technique of least-squares approximation.

The reason for tracking the fourth, fifth, sixth, and seventh reflections is that these images are of high quality and provide large magnification of the surface slope deformations. From the discussion in Section 3 it can be readily shown that a surface slope deformation of $\Delta\theta$ produces a $2mf\Delta\theta$ lateral shift of the m th reflection spot, where f is the focal length of the convergent imaging lens. With the position shifts of the four spots in written vector notation, a surface slope deformation would produce shifts in the reflection spots proportional to vector $\langle 8f, 10f, 12f, 14f \rangle$. The constant shifts due to noise sources (3) and (4), on the other hand, produce motions proportional to the vector $\langle f, f, f, f \rangle$ because all the spots are shifted identically. One can calculate the angle between any two vectors by taking the inverse cosine of the dot product of the normalized vectors. Performing this computation, one would find that the angle between $\langle 8f, 10f, 12f, 14f \rangle$ and $\langle f, f, f, f \rangle$ is $\sim 11.5^\circ$. In other words, these two vectors are nearly collinear (or indistinguishable), making the least-squares fit susceptible to noise fluctuations.⁷ To alleviate this problem, we rearrange the system so that two sets of reflection spots, one from the reference cavity and one from a chosen cavity, appear on the CCD camera simultaneously. We again denote the motion in vector notation, where the first four elements correspond

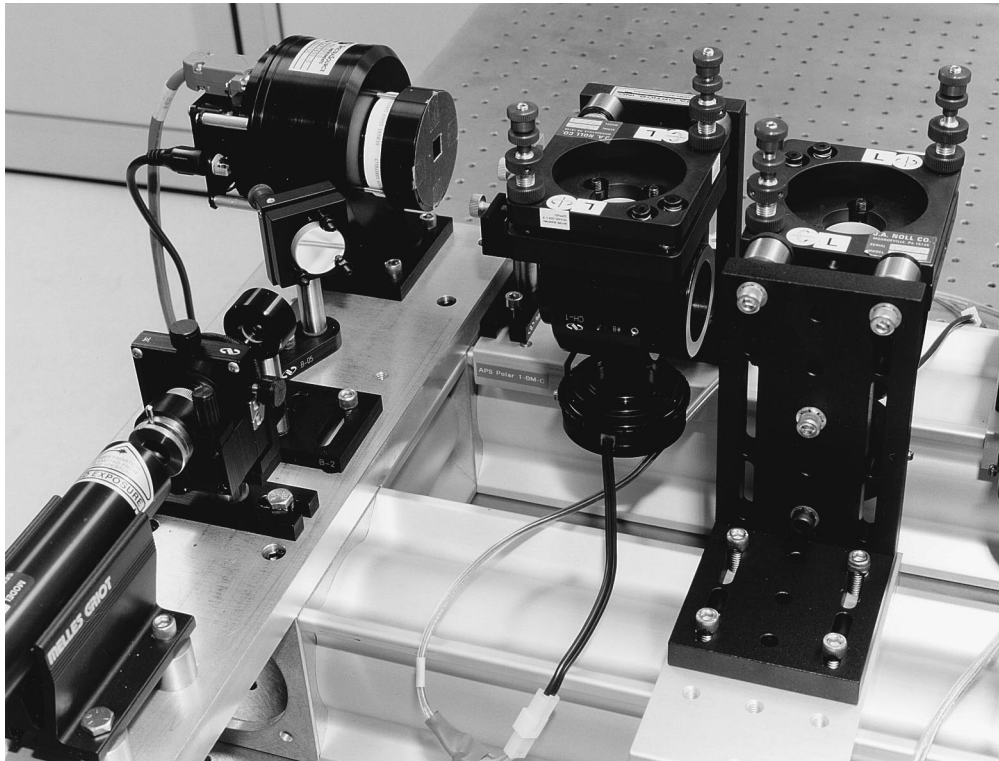


Fig. 4. Two (out of eight) cavities of the actual surface metrology unit built with off-the-shelf commercially available components.

to the fourth, fifth, sixth, and seventh reflections from one site, and the last four elements correspond to those from the other site. A deformation in the first site would then produce shifts in the reflection spots given by $\langle 8f, 10f, 12f, 14f, 0, 0, 0, 0 \rangle$ (with no influence on the other site). Similar reasoning shows that the motion vector $\langle 0, 0, 0, 0, 8f, 10f, 12f, 14f \rangle$ is the effect of a deformation in the second site, and $\langle f, f, f, f, f, f, f, f \rangle$ is that of a constant shift due to noise sources (3) and (4).

Now, the angles between these eight-element vectors are at least 45° : 90° between the $\langle 8f, 10f, 12f, 14f, 0, 0, 0, 0 \rangle$ and $\langle 0, 0, 0, 0, 8f, 10f, 12f, 14f \rangle$ vectors, 46.1° between the $\langle 0, 0, 0, 0, 8f, 10f, 12f, 14f, 0 \rangle$ and $\langle f, f, f, f, f, f, f, f \rangle$ vectors, and 46.1° between the $\langle 8f, 10f, 12f, 14f, 0, 0, 0, 0 \rangle$ and $\langle f, f, f, f, f, f, f, f \rangle$ vectors. These basis vectors are quite distinct; hence the projections of a data vector onto these vectors are much less susceptible to measurement noise. It can readily be shown using linear algebra that the best estimate, in the least-squares sense, for surface slope deformations at the two observed sites is then given by the first two elements of the vector,⁶

$$r = (A \cdot A^T)^{-1} \cdot A \cdot x^T, \quad (1)$$

where x is the row vector of measured shifts and A is the matrix defined as follows:

$$A = \begin{bmatrix} 8f & 10f & 12f & 14f & 0 & 0 & 0 & 0 \\ 0 & 0 & 0 & 0 & 8f & 10f & 12f & 14f \\ f & f & f & f & f & f & f & f \end{bmatrix}. \quad (2)$$

Now, with the least-squares technique, one can accurately determine the constant shift and the two independent deformations.

5. Test Results

A photograph of the actual metrology unit is shown in Fig. 4. The entire unit, excluding the computer, weighs less than 100 lbs. Almost all the hardware is off-the-shelf commercial components. The cavity units are mounted on rails to accommodate different mirror tank designs. The interface and image analysis software are written to operate in Microsoft Windows for user friendliness.

The dynamic range of the system is approximately $30 \mu\text{rad}$, limited by the size of the CCD detector. After an initial settling down period of 30 min the long-term stability is approximately $\pm 1 \mu\text{rad}$, peak-to-peak, over a period of more than 15 h. To demonstrate this, two small test mirrors were set up, one for reference and one to probe. The metrology unit was then turned on to perform measurements for approximately 15 h (with the shutters opening and closing). Lights and fans in the laboratory were turned off, and room temperature was kept constant to within 2°F . With the mirrors unperturbed, the measured fluctuation profiles are shown in Fig. 5. Note that the short-term stability is only $\sim 0.3 \mu\text{rad}$ (zero-to-peak) over any 10-min period. This random fluctuation typically limits the system resolution to $\sim 0.5 \mu\text{rad}$. To further illustrate this, two piezoelectric translators were added to tilt the sample mirror as measurements were taken. These

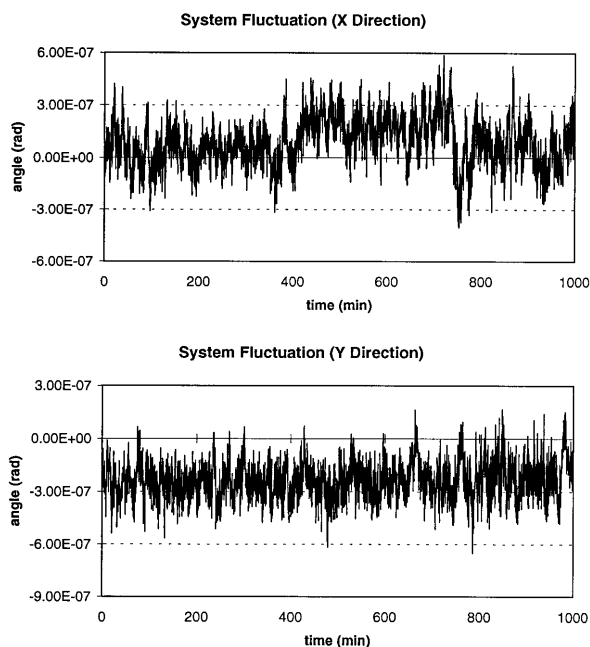


Fig. 5. Fluctuations of the surface metrology unit when probing the unperturbed test mirror. The two profiles, one for the x direction and one for the y direction, were taken over a period of more than 15 h.

results are shown in Fig. 6. For each positive step jump seen in the profile, the voltage across each piezoelectric translator has been increased by 1 V. (Because of the nonlinear response of the piezoelectric crystal, the motion jumps are not uniform, even though the voltage jumps are.) Fluctuations greater than $0.3 \mu\text{rad}$ within each step are probably due to the transient effects of the piezoelectric crystals. The kinetic mount for the test mirror is oriented so that an equal expansion on both crystals produces tilts predominantly along the y direction. The small tilts seen along the x direction are probably due to motion coupling inherent in the mount design or the slight difference in the voltage responses of the crystals. Also, notice that, because

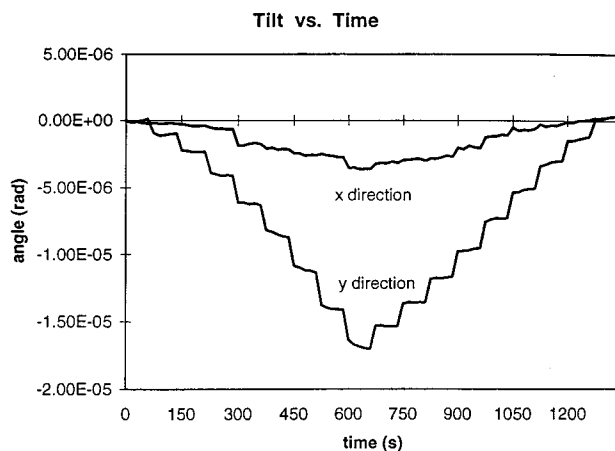


Fig. 6. Tilt measurements of the test mirror as 1-V steps are applied to the piezoelectric translators that tilt the mirror.

of the hysteresis in the piezoelectric crystal, a voltage decrease of 7 V after a voltage increase of 7 V does not drive the mirror back to its exact original location. Nevertheless, the average responsivity of $2.2 \mu\text{rad}/\text{V}$ is well within tolerance of the calculated value for our piezoelectric translator and mount setup.

6. Extension to Adaptive Optics

Currently our system is capable of sampling eight surface points in ~ 1.7 min. With the fast Pentium-based personal computer, the main speed limitation is the transfer rate of the CCD camera. Much improvement and price reductions in CCD technology have occurred since the camera was purchased a year ago. Currently available CCD cameras can reduce the acquisition time by more than a factor of 2. With a faster sampling rate, one can imagine placing actuators behind each probing site and closing the feedback loop with the monitoring system to form an adaptive mirror system for a broad range of applications. We have performed experiments that demonstrated that step errors can easily be corrected with a simple proportional feedback and piezoelectric actuators. We are currently experimenting with proportional-derivative feedback for correcting ramp errors. Although the deformation rate of the mirror surface under high heat load has not been measured yet, we feel confident that, even with the current sampling time of 1.7 min, a successful adaptive optics system for synchrotron or other applications can be easily realized with our system.

7. Conclusion

In this paper a noncontact metrology system capable of real-time, *in situ* monitoring of synchrotron mirror surfaces under high heat load is described. Although the metrology system was conceived with this particular application in mind, it is obvious that the unit can be used in other applications in which continuous *in situ* monitoring of the optical surface is desirable. The prototype system has been tested on sample optics, and those results are very promising. Preparations are under way to test the system on an actual synchrotron mirror in operation. Finally, we are currently investigating the possibility of incorporating the metrology unit into an adaptive mirror system.

This work is supported by the U.S. Department of Energy—Basic Energy Sciences under contract W-31-109-ENG-38.

References

1. S. Qian, W. Jark, P. Z. Takacs, K. J. Randall, and W. B. Yun, "In situ profiler for high heat load mirror measurement," *Opt. Eng.* **34**, 396–402 (1995).
2. J. Susini, R. Baker, M. Krumrey, W. Schwegle, and Å. Kvik, "Adaptive x-ray mirror prototype: first results," *Rev. Sci. Instrum.* **66**, 2048–2052 (1995).
3. D. Malacara, *Optical Shop Testing* (Wiley, New York, 1978), Chap. 7, p. 252.

4. R. S. Sirohi and M. A. Kothiyal, *Optical Components, Systems, and Measurement Techniques* (Marcel Dekker, New York, 1991), Chap. 5, p. 187.
5. M. V. Klein and T. E. Furtak, *Optics* (Wiley, New York, 1989), Chap. 3, p. 151.
6. A. V. Oppenheim and R. W. Schaffer, *Discrete-Time Signal Processing* (Prentice Hall, New York, 1989), Chap. 7, p. 464.
7. J. G. Pronkis, C. M. Rader, F. Ling, and C. L. Nikias, *Advanced Digital Signal Processing* (Macmillan, New York, 1992), Chap. 5, p. 267.